Biochimica et Biophysica Acta, 769 (1984) 370–376
Elsevier

BBA 71933

DIELECTRIC DISPERSION OF A SINGLE SPHERICAL BILAYER MEMBRANE IN SUSPENSION

KOJI ASAMI and AKIHIKO IRIMAJIRI

Department of Physiology, Kochi Medical School, Nankoku, Kochi 781-51 (Japan)

(Received August 5th, 1983)

Key words: Lipid bilayer; Monooleyl phosphate; Dielectric behavior; Membrane capacitance

Single spherical bilayer membranes of the Pagano-Thompson type (Pagano, R. and Thompson, T.E. (1967) Biochim. Biophys. Acta 144, 666–669), formed from monooleyl phosphate and cholesterol dissolved in $CHCl_3/CH_3OH/n$-decane, were subjected to a fast impedance analysis of high precision. Dielectric behavior of the whole system, as monitored from outside the spherical membrane, was sensitive to changes in the membrane state from the thick colored to the thin black state. With a spherical membrane 2–3 mm in diameter formed in the sample cavity containing 0.12 ml 10 mM NaCl, the former state was characterized by a dielectric dispersion having dielectric increment ($\Delta\epsilon$) of some 10^2 and characteristic frequency (f_c) around 10^6 Hz, while the latter had $\Delta\epsilon \simeq 10^5$ and $f_c \simeq 10^3$ Hz. Complex plane plots for both dispersions traced semicircles, indicating that the present system may be unequivocally analyzed to yield spherical radius and membrane capacity (C_m) on the basis of a well-established dielectric theory. C_m for the thin membranes has thus been determined to be 0.54 $\mu F \cdot cm^{-2}$, in excellent agreement with a separate determination on planar membranes. The applicability of the present type of spherical membranes under dielectric monitoring to the study of membrane fusion or of exocytosis is suggested.

Introduction

The relative permittivity (or dielectric constant) of a suspension of cells and vesicles varies as the frequency of applied field is varied, a phenomenon termed 'dielectric dispersion'. The majority of such dispersions are observed in the radio-frequency region and hence interpreted as basically due to interfacial polarization, to which the presence of the demarcating membrane is essential. Then it is not only expected but actually feasible to extract from observed dispersion data some membrane-related parameters, e.g., membrane capacity (C_m), if we are provided with an appropriate dielectric model for the system under study.

One such model of current use, developed by Pauly and Schwan [1], implies that a variety of spherical cells can be approximated by a shelled sphere (Fig. 1a) and that the complex permittivity (ϵ^*) of the suspension of these spheres may be represented by

$$\epsilon^* = \epsilon_h + \frac{\Delta\epsilon}{1 + j\omega\tau} + \frac{\kappa_l}{j\omega\epsilon_v} \quad (1)$$

Here, ϵ and κ are respectively relative permittivity and conductivity for the suspension; subscripts l and h refer to the limiting values at low and high frequencies, respectively; $\Delta\epsilon$ = dielectric increment ($\epsilon_l - \epsilon_h$), ϵ_v = permittivity of vacuum, τ = relaxation time, ω = angular frequency, and $j = (-1)^{1/2}$. Eqn. 1 has been derived using the condition that $\kappa_s/\kappa_a \ll d/R \ll 1$ and $\kappa_s/\kappa_i \ll d/R \ll 1$ (notations defined as in Fig. 1a), which appears to be valid for most living cells in suspension.

By putting $\epsilon^* - \kappa_l/j\omega\epsilon_v = \epsilon' - j\epsilon''$ and combining it with Eqn. 1 we have

$$(\epsilon' - \epsilon_h - \Delta\epsilon/2)^2 + (\epsilon'')^2 = (\Delta\epsilon/2)^2 \quad (2)$$

0005-2736/84/$03.00 © 1984 Elsevier Science Publishers B.V.

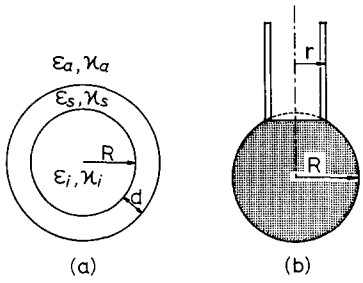

Fig. 1. (a) A dielectric model of the spherical membrane separating two aqueous phases. ϵ and κ are, respectively, relative permittivity and conductivity for three phases comprising the system, viz., suspending medium (denoted by subscript a), membrane (by subscript s) and inside solution (by subscript i). (b) A spherical membrane of radius R protruded from the tip of a plastic tubing of outer diameter $2r$.

which implies that the plots of ϵ'' vs. ϵ' trace a semicircle with its center located on the abscissa. In the practical case of biological cell suspensions, however, our commonest experience is such that the observed points better fit a circular arc having depressed center rather than a semicircle. According to the phenomenology of dielectric theories [2] the dispersions represented by the circular arcs may be characterized in terms of a more-or-less broadened spectrum of relaxation times, while those represented by the semicircles have only one relaxation time for each dispersion as formulated in Eqn. 1. Broadening of the relaxation spectrum with respect to the cell suspensions has been attributed to several factors: (i) non-sphericity in cell shape [3,4], (ii) multilamellar structure of the membrane phase [5–7], (iii) frequency-dependent properties of the membrane and/or the core phase [8], (iv) intercellular heterogeneity with respect to the electric and morphometric properties of cells [9], (v) concentrated suspension of homogeneous cells [10], and last but not least (vi) uncontrolled instrumental errors.

Problems due to these factors, singly or in combination, often emerge and hinder the unequivocal interpretation of dielectric studies on living cells. This awareness has prompted us to carry out measurements with a single, spherical, bilayer lipid membrane suspended in, and containing, well-defined aqueous salt solutions. In the present paper we first describe the bilayer formation process as monitored by a dielectric dispersion technique, and second offer evidence for an excellent agreement between theory and experiment with the simplest available model system. This two-fold observation indicates that our method could find a wider application to other fields of membrane studies.

Materials and Methods

Formation of membranes

The membrane-forming solution was prepared by dissolving 20 μmol monooleyl phosphate (synthesized by Dr. Tsuji, Kao Soap Co., Japan) and 5 μmol cholesterol in 1 ml mixture of chloroform/methanol/*n*-decane (4 : 3 : 3, v/v). The procedure for formation of spherical membranes was a modification of Pagano and Thompson [11] or of Breisblatt and Ohki [12]; our membranes were of a hanging type instead of a floating type. Briefly, a Gilson micropipetter (Model P20) fitted with a polyethylene tube was first filled up with an inside solution, followed by a very small amount (0.2–0.5 μl) of the membrane-forming solution, and then the tip of the tubing was inserted in the dielectric cell (Fig. 2) that had been also filled with the same salt solution as the inside one. Careful discharge of the inside solution resulted in bulging of a spherical lipid membrane, which was left to thin down spontaneously.

Planar bilayer membranes were made from the same membrane-forming solution by a conventional brush method. Unless otherwise specified, these two types of membrane were formed in an unbuffered 10 mM NaCl solution at room temperature (21–23°C).

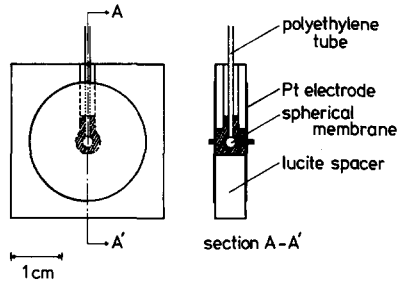

Fig. 2. The cell used for dielectric measurements of the spherical membrane system. Volume of the sample cavity and cell constant are 118 μl and 28 fF, respectively.

Dielectric measurements

Fig. 2 shows the design of the dielectric cell used. This is essentially a parallel plate condenser consisting of a lucite spacer with a hole as the sample cavity and a pair of platinized Pt electrodes glued to the spacer. Admittances of the cell assembly, as a function of applied frequency, were measured semi-automatically with an impedance analyzer (model 4192A, Yokogawa-Hewlett-Packard Co., Japan) that was controlled by a desk-top computer (model 9825S, Hewlett-Packard Co., U.S.A.). The use of this system enabled us to scan over 121 frequency points in the log-linear range of 10^1–10^7 Hz within 2.5 min even when the 'average' mode of operation was employed. Every set of raw data was corrected for the residual inductance effect according to the method of Schwan [13]. The final values of relative permittivity and conductivity thus obtained were immediately plotted as a dispersion diagram or stored for further analysis.

Analysis of Data

By definition, complex permittivity takes the form $\epsilon^* = \epsilon + \kappa/j\omega\tau\epsilon_v$, so that comparison with Eqn. 1 yields the phenomenological expressions for ϵ and κ:

$$\epsilon = \epsilon_h + \Delta\epsilon/\left[1+(f/f_c)^2\right] \tag{3}$$

$$\kappa = \kappa_l + \Delta\kappa(f/f_c)^2/\left[1+(f/f_c)^2\right] \tag{4}$$

where $\Delta\epsilon = \epsilon_l - \epsilon_h$, $\Delta\kappa = \kappa_h - \kappa_l = \epsilon_v\Delta\epsilon/\tau$, and $f/f_c = \omega\tau$.

On the other hand, some of the phenomenological parameters have been correlated with the phase parameters included in the shell model (Fig. 1a) through the relations [1,14]:

$$\kappa_l/\kappa_a = 2(1-P)/(2+P) \tag{5}$$

$$\frac{\kappa_h}{\kappa_a} = \frac{(1+2P)\kappa_i + 2(1-P)\kappa_a}{(1-P)\kappa_i + (2+P)\kappa_a} \tag{6}$$

$$\tau = \frac{1}{2\pi f_c} = RC_m\left(\frac{1}{\kappa_i} + \frac{1}{\kappa_a}\cdot\frac{1-P}{2+P}\right) \tag{7}$$

$$\Delta\epsilon = 9RC_mP/(2+P)^2\epsilon_v \tag{8}$$

where P is the volume fraction and C_m is membrane capacity defined by

$$C_m = \epsilon_s\epsilon_v/d \tag{9}$$

Combination of Eqns. 5 and 6 to eliminate κ_a leads to

$$\Delta\kappa\left[(2+P)^2/\kappa_i + 2(1-P)^2/\kappa_l\right] - 9P = 0 \tag{10}$$

Also from an elementary algebra, volume (v') for the shaded portion of Fig. 1b is given by

$$v' = (\pi/3)R^3\left[2+\left(2+(r/R)^2\right)\sqrt{1-(r/R)^2}\right] \tag{11}$$

where r/R is ratio of radii for the tube and the spherical membrane suspended therefrom.

Determination of P and R

To begin with, let us define a volume fraction, P', such that

$$P' = v'/V \tag{12}$$

where V is volume of the sample cavity ($= 118\ \mu l$) without the tube inserted. As a direct volumetric determination of v' was found to be insufficiently accurate, we employed the following relation, which is analogous to Eqn. 10, for the determination of P′ values:

$$\Delta G\left[(2+P')^2/K\kappa_i + 2(1-P')^2/G_l\right] - 9P' = 0 \tag{13}$$

where G values denote conductances measured with the membrane system in situ, K is the cell constant, and the other symbols are as defined above. With the same solution used both for the inside compartment and for the outside, P' could also be evaluated through $G_l/G_a = 2(1-P')/(2+P')$, which is analogous to Eqn. 5, where G_a is conductance in situ after withdrawal of the membrane. Both approaches gave a consistent result; accordingly, we preferred the approach using Eqn. 13 because of its competence for the case of $\kappa_a \neq \kappa_i$. With the P' thus obtained we can calculate the spherical radius R from Eqns. 11 and 12 provided with known values of r and V. Once R is known, evaluation of P, the volume fraction of the spherical model (Fig. 1a), is straightforward, since $P = 4\pi R^3/3V$.

Determination of apparent membrane capacity (C_m)

Membrane capacity can be calculated by using either Eqn. 7 or Eqn. 8. The former approach requires the knowledge of f_c and the latter that of $\Delta\epsilon$, both being observable from the dielectric measurements. However, the values of C_m so obtained were apparent in that the tip of the tubing certainly masked the *cap* portion of an ideal sphere from the applied field (Fig. 1b). Hence, the final estimate of C_m was obtained by extrapolation to $r/R = 0$.

Results and Discussion

Fig. 3 shows a typical experiment to chase the time-course of membrane thinning in our system. Immediately after bulging the membrane to a volume of approx. 10 μl, we started scanning the frequency of the applied field (f) up towards 10 MHz while recording both ϵ and κ for the whole

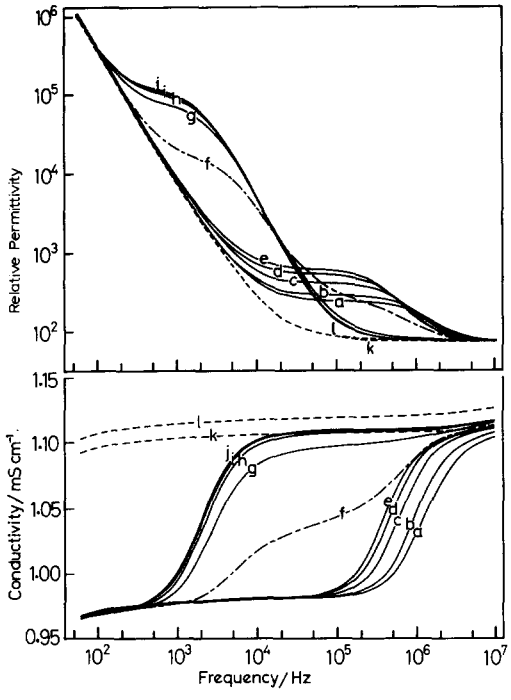

Fig. 3. Time-dependent changes of dielectric dispersion curves for a single, spherical membrane separating an identical solution of 10 mM NaCl. Paired curves a represent the first scan immediately after bulging the membrane; curves b–j were recorded successively, in this order, at intervals of 3.2 min. Curves k refer to withdrawal of the membrane, curves l to removal of the tubing from the cell.

suspension as a function of f. It took about 2.5 min for a single scanning to cover the entire range. The result of this first scanning is depicted as the paired curves marked 'a'. Repeated scannings thereafter, at intervals of 3.2 min, gave rise to the dispersion curves b–j. Curves j represent the final steady state. Curves a–e in Fig. 3, characterized by both relatively small $\Delta\epsilon$ and high f_c values, indicate that the membrane was premature and still in a thick state, as will be detailed in the numerical analysis (Table I). 15 min or so after bulging, the magnitude of $\Delta\epsilon$ increased abruptly with a concomitant lowering of f_c from the megahertz down to the kilohertz region (curves f, Fig. 3). This transition occurred so rapidly relative to the scanning time that curves f might not have reflected one and the same state of the membrane. Approx. 20 min after bulging, the dispersions shifted to the lower-kilohertz region and stayed there with no further changes in ϵ and κ, indicating that the membrane thinning was almost complete.

Fig. 4 illustrates the complex plane plots of data in Fig. 3. Excepting the lower frequencies wherein the measurements were affected by electrode polarization, the observed points fit well with semicircles just as expected from Eqn. 2. The limiting values of ϵ and κ estimated from these circular plots are listed in Table I. It may be relevant to note here again that the membrane state named f gave rise to an apparently anomalous trace in Fig. 4a, indicating coexistence of the thick and thin portions on the same spherical surface. This inference comes from the direction of time-chase employed; that is, every scanning was made towards the higher-frequency side and never in the reverse direction. Table I summarizes the numerical results, from which those for state f are omitted for the reason above. It is clear from the table that the spherical membrane after bulging underwent a transition from the thick state having a C_m of a few nF/cm^2 to the thin, black membrane state having a C_m as high as 0.4–0.5 μF/cm^2.

In the second series of experiment we reduced the spherical size by stepwise withdrawals from the inside solution after the complete thinning of the membrane was attained. The results are compiled in Figs. 5 and 6 as well as in Table II. Again, fitting to the 'semicircle' rule has been confirmed. The C_m values calculated from Eqn. 7 or Eqn. 8

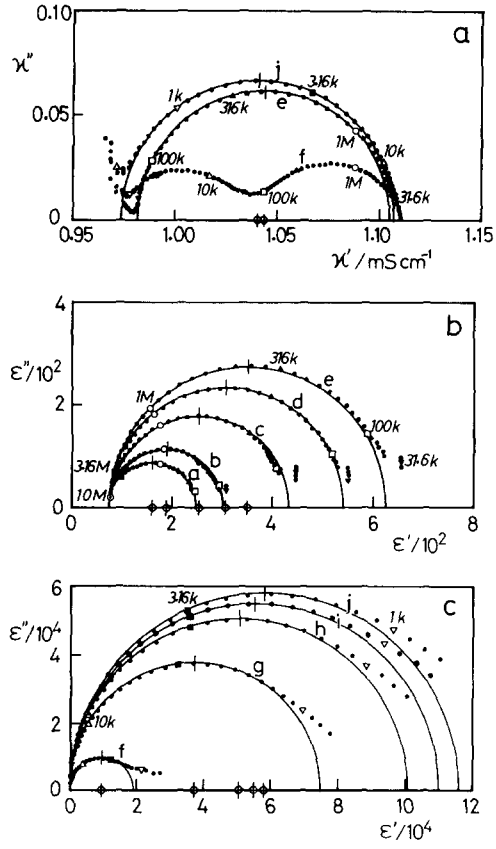

Fig. 4. Complex plane plots of data in Fig. 3. The number on each symbol refers to marker frequency; the vertical bar to characteristic frequency. Note that the scale is different between Fig. 4b and Fig. 4c.

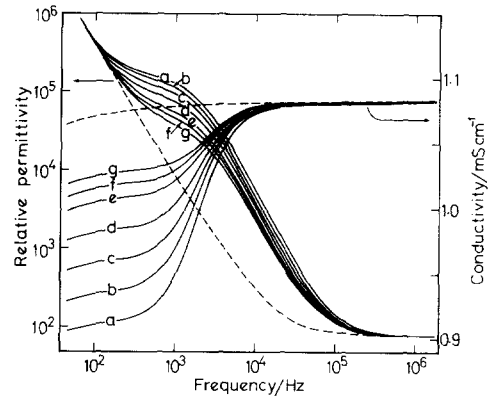

Fig. 5. Volume dependence of dispersion profiles, as determined with an identical spherical bilayer membrane system containing, and suspended in, 10 mM NaCl. Curves a represent the membrane bulged to a maximum volume. Curves b–g refer to the spherical membranes after successive reduction in volume. Broken lines, no membrane.

agree very well with each other.

As mentioned in Materials and Methods, our membranes were not ideally spherical but devoid of the *cap* portion that was in contact with the tip of the polyethylene tube. This fact must have affected the determination of C_m. In order to determine C_m values free from this effect, measurements were made with three different tube diameters while changing the spherical radius, R, as widely as possible. The apparent values of C_m are

TABLE I

SPHERICAL MEMBRANE THINNING AS REFLECTED IN MEMBRANE CAPACITY CHANGES

$C_m(\Delta\epsilon)$ and $C_m(f_c)$ were calculated from Eqns. 8 and 7, respectively. $\kappa_a = \kappa_i = 1.119$ mS/cm, $\kappa_h = 1.107$ mS/cm, and $\epsilon_h = 76$. Data are from Figs. 3 and 4.

Membrane state	Dielectric parameters			P	R (mm)	Membrane capacity (μF/cm^2)	
	ϵ_i	κ_i (mS/cm)	f_c (kHz)			$C_m(\Delta\epsilon)$	$C_m(f_c)$
a	250		1200			$0.72\cdot10^{-3}$	$0.78\cdot10^{-3}$
b	303		950			$0.94\cdot10^{-3}$	$0.99\cdot10^{-3}$
c	432	0.981	620	0.0787	1.30	$1.48\cdot10^{-3}$	$1.52\cdot10^{-3}$
d	532		480			$1.89\cdot10^{-3}$	$1.97\cdot10^{-3}$
e	624		400			$2.27\cdot10^{-3}$	$2.36\cdot10^{-3}$
f	–	–	–	–	–	–	–
g	$74.4\cdot10^3$		2.75			0.288	0.338
h	$100.8\cdot10^3$	0.974	2.32	0.0831	1.33	0.390	0.400
i	$109.8\cdot10^3$		2.18			0.424	0.426
j	$115.8\cdot10^3$		2.05			0.448	0.453

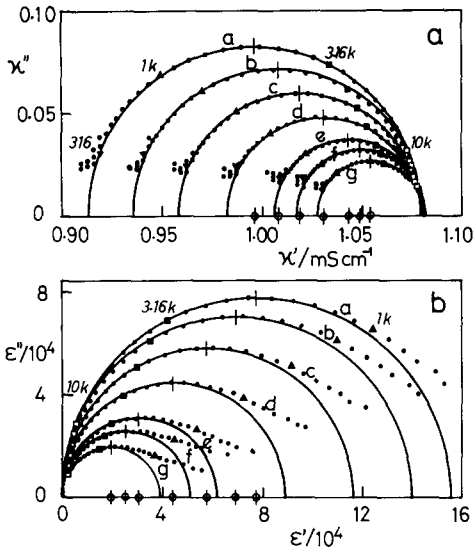

Fig. 6. Complex plane plots of data in Fig. 5. The number on each symbol refers to marker frequency; the vertical bar indicates characteristic frequency.

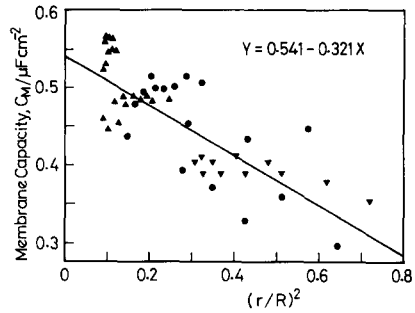

Fig. 7. Plots of 'apparent' C_m, as a function of $(r/R)^2$, calculated from Eqn. 8. Data obtained by using three different tubes of diameter (in mm), 0.8 (▲), 1.1 (●) and 1.6 (▼), were pooled to give a linear regression as indicated. Correlation coefficient = −0.786, S.E.(slope) = 0.036, S.E.(intercept) = 0.011, and $n = 50$.

plotted in Fig. 7 as a function of $(r/R)^2$; here C_m refers to that calculated from Eqn. 8. An estimate of 0.541 μF/cm^2 for the bilayer membrane capacity could be read from the Y-intercept of the regression line. Another trial of calculation based on Eqn. 7 resulted in a linear regression, $Y = 0.541 - 0.260\ X$ (S.E. for Y-intercept = 0.011, $n = 50$). Thus, both calculations gave the same result, $C_m = 0.54$ μF/cm^2 for $r = 0$. This figure compares favorably with a C_m value * of 0.517 ± 0.004 μF/cm^2 (mean ± S.E., $n = 15$) which was obtained from a separate measurement on the planar bilayers formed from the same membrane-forming solution.

Preliminary results on the present 'millimeter-sized' spherical bilayers further indicate that: (i) the dielectric behavior of the one-sphere system such as described here was equally predictable from Eqn. 1 or from Eqn. 2 (i.e., the semicircle type) even when $\kappa_i \neq \kappa_a$; (ii) the two-sphere system, in which a second sphere of radius R_2 was formed through a separate tubing inserted in parallel with the first, gave semicircle plots on the complex plane as long as the two internal solutions were identical ($\kappa_{i1} = \kappa_{i2}$); and (iii) the two-sphere system having different internal conductivities ($\kappa_{i1} \neq \kappa_{i2}$), by contrast, gave rise to definitely broadened dispersion curves (i.e., the circular arc type).

The results presented, taken together, demonstrate that the single, spherical, bilayer lipid membranes show a lucid dielectric behavior, hence enabling an unequivocal analysis of the dispersion data, and that the membrane capacity itself is frequency independent as reflected by the 90° phase angles on the Cole-Cole plot. Clearly, such a lucidity or simplicity cannot always be expected in the practice of biological dielectric measurements using cell suspensions, since heterogeneity in cellular structure and/or composition is more or less inevitable even if a single cell species is employed. One way of circumventing this problem would certainly be to make measurements on isolated single cells as was long ago initiated by Cole and co-workers (for review, see Ref. 8). To the authors' knowledge, however, very few other than Cole's group (on egg cells) have pursued the single-cell approach to the membrane impedance studies. By taking advantage of our methodology here described, a long-term (i.e., up to 10 days), continu-

* The planar bilayer membrnes were formed on a hole of 1.585 mm diameter perforated through a 0.2 mm thick Teflon septum. With our membrane-forming solution, the so-called 'torus' was not observed even with the aid of a moderate power telescope, so we calculated the C_m values on the basis of the hole diameter as determined. Accordingly, the C_m of 0.517 μF/cm^2 is a lower limit; if, however, there existed a torus of 20 μm width, then the calculated C_m should be 0.544 μF/cm^2.

TABLE II

APPARENT MEMBRANE CAPACITY AS A FUNCTION OF SPHERICAL SIZE

$C_m(\Delta\epsilon)$ and $C_m(f_c)$ were calculated from Eqns. 8 and 7, respectively. $\kappa_a = \kappa_i = 1.092$ mS/cm, $\kappa_h = 1.079$ mS/cm and $\epsilon_h = 77$. Data are from Figs. 5 and 6.

Membrane	Dielectric parameters			P	R (mm)	Membrane capacity (μF/cm^2)	
	$\epsilon_l(\times 10^{-3})$	κ_l (mS/cm)	f_c (kHz)			$C_m(\Delta\epsilon)$	$C_m(f_c)$
a	155	0.913	1.91	0.108	1.45	0.435	0.440
b	140	0.936	1.83	0.0918	1.37	0.478	0.481
c	115.5	0.959	1.84	0.0768	1.29	0.493	0.504
d	88.0	0.983	1.96	0.0614	1.20	0.498	0.506
e	60.8	1.007	2.14	0.0458	1.09	0.501	0.507
f	51.0	1.017	2.20	0.0392	1.03	0.513	0.517
g	39.4	1.028	2.38	0.0326	0.97	0.504	0.507

ous, dielectric monitoring of the oocyte growth is currently underway in our laboratory. Finally, it seems also promising to apply the method to membrane fusion phenomena in which externally added cells or vesicles are allowed to fuse with the basal spherical bilayer to alter its surface area and electrical parameters such as C_m, both being detectable, if any.

Acknowledgements

We wish to thank Dr. T. Hanai, Kyoto University, for pertinent discussion. This work was supported by grant from The Ministry of Education, Science and Culture, Japan.

References

1 Pauly, H. and Schwan, H.P. (1959) Z. Naturforsch. 14B, 125–131
2 Cole, K.S. and Cole, R.H. (1941) J. Chem. Phys. 9, 341–351
3 Asami, K., Hanai, T. and Koizumi, N. (1980) Jpn. J. Appl. Phys. 19, 359–365
4 Asami, K., Hanai, T. and Koizumi, N. (1980) Biophys. J. 31, 215–228
5 Fricke, H. (1955) J. Phys. Chem. 59, 168–170
6 Irimajiri, A., Doida, Y., Hanai, T. and Inouye, A. (1978) J. Membrane Biol. 38, 209–232
7 Irimajiri, A., Hanai, T. and Inouye, A. (1979) J. Theor. Biol. 78, 251–269
8 Cole, K.S. (1968) Membranes, Ions and Impulses, pp. 6–59, University of California Press, Berkeley
9 Irimajiri, A., Hanai, T. and Inouye, A. (1975) Biophys. Struct. Mechan. 1, 273–283
10 Hanai, T., Asami, K. and Koizumi, N. (1979) Bull. Inst. Chem. Res. Kyoto Univ. 57, 297–305
11 Pagano, R. and Thompson, T.E. (1967) Biochim. Biophys. Acta 144, 666–669
12 Breisblatt, W. and Ohki, S. (1975) J. Membrane Biol. 23, 385–401
13 Schwan, H.P. (1963) in Physical Techniques in Biological Research (Nastuk, W.L., ed.), Vol. 6B, pp. 323–407, Academic Press, New York
14 Hanai, T. (1968) in Emulsion Science (Sherman, P., ed.), Ch. 5, Academic Press, London